Journal of Organometallic Chemistry 695 (2010) 721–729

Contents lists available at ScienceDirect

Journal of Organometallic Chemistry

journal homepage: www.elsevier.com/locate/jorganchem

Influence of the basicity of internal bases in diiron model complexes on hydrides formation and their transformation into protonated diiron hexacarbonyl form

Zhiyin Xiao [a], Fenfen Xu [a], Li Long [a], Yinqiu Liu [c], Giuseppe Zampella [b,*], Luca De Gioia [b], Xirui Zeng [c], Qiuyan Luo [c], Xiaoming Liu [a,*]

[a] Department of Chemistry, Institute for Advanced Study, Nanchang University, Nanchang 330031, China
[b] Department of Biotechnology and Biosciences, University of Milano-Bicocca, 20126 Milano, Italy
[c] School of Chemistry and Chemical Engineering, Jinggangshan University, Ji'an 343009, China

ARTICLE INFO

Article history:
Received 27 September 2009
Received in revised form 4 December 2009
Accepted 11 December 2009
Available online 16 December 2009

Keywords:
[FeFe]-hydrogenase
Model complex
Internal base
Bridging hydride
DFT calculation

ABSTRACT

Reaction of 2-(1-(pyridin-2-yl)ethyl)propane-1,3-dithiol with tri-iron dodecacarbonyl afforded a diiron pentacarbonyl complex, $[Fe_2\mathbf{L}(CO)_5]$ (**A** and $\mathbf{H_2L}$ = 2-methyl-2-(1,2,5,6-tetrahydropyridin-2-yl)propane-1,3-dithiol). In the reaction, the pyridinyl ring of the original ligand was partially hydrogenated during the reaction. This complex was fully characterised by using crystallographic, infrared, and NMR spectroscopic techniques. Formation reaction of its bridging hydride and subsequent conversion into its protonated diiron hexacarbonyl complex, $[Fe_2\mathbf{L}(CO)_6]$ ($\mathbf{ACOH^+}$ in which the N atom of **L** is decoordinated and protonated), were experimentally and theoretically investigated. Results for this complex alongside with theoretic investigations into other diiron pentacarbonyl analogues revealed positive correlation of basicity of the internal bases of these investigated complexes to bridging hydrides formation. But subsequent conversion of these bridging hydrides into protonated diiron hexacarbonyl complexes was not solely dictated by the basicity. Protophilicity of the internal base and lability of its coordination with the diiron centre play also an important role as revealed by experimental and theoretic investigations.

1. Introduction

In the past decade, bio-inspired chemistry related to the [FeFe]-hydrogenase [1–2] has attracted tremendous attentions due to its relevance to the production of hydrogen, a possible future clean energy source. Albeit it is still a long journey before achieving artificial systems with efficiency comparable to the metalloenzyme, significant progresses have been made in recent years. These achievements embraced all aspects of the bioinorganic chemistry related to this enzyme [3–26], ranging from structural mimics to mechanistic understandings of the enzymatic catalysis.

In the catalysis of hydrogen evolution, mechanisms of proton transfer, hydride formation, and its conversion, have fundamental importance in understanding the enzymatic catalysis, devising, and synthesising novel artificial systems. Although there are many reports concerning hydride chemistry in modelling the diiron subunit of the H-cluster of the hydrogenase [6,10,27–33], reports describing interactions of bridging hydride with internal pendant base in either the first or second coordinating environment are rare. Recently, Wang, Sun and their co-workers observed that a bridging hydride interacts significantly with a pendant base group in a diiron model complex [34]. Talarmin and his co-workers reported an inter-conversion between a bridging hydride and a pendant base in the second coordinating environment in dichloromethane [35]. Earlier, we reported some diiron pentacarbonyl complexes with an internal base as models for the sub-unit of the enzyme, which, unlike the above systems reported, was bound to one of the iron atoms with some lability, $[Fe_2\mathbf{L'}(CO)_5]$ ($\mathbf{H_2L'}$ = a tridentate ligand with two S ligating atoms and a N-containing base) [36]. Their protonation proceeded in two pathways. The bound base dissociated into a pendant internal base, which was subsequently protonated and diiron hexacarbonyl complex formed consequently by taking up a CO molecule. This pathway is particularly favoured under CO atmosphere. The Fe–Fe bond could also be protonated to form first a bridging hydride, which at the end could transform into a diiron hexacarbonyl complex as shown in Scheme 1 [36].

The formation of bridging hydrides shown in Scheme 1 was mainly confirmed by using infrared spectroscopy. Their NMR resonances were elusive due to their instability while a thioether analogue, $[Fe_2(\mu\text{-}SCH_2)_2CMe(CH_2SMe)(CO)_5]$ [8,37], was stable enough

* Corresponding authors. Tel./fax: +86 (0) 791 3969254 (X. Liu), tel.: +39 (0) 264483416; fax: +39 (0) 264483478 (G. Zampella).
E-mail addresses: giuseppe.zampella@unimib.it (G. Zampella), xiaoming.liu@ncu.edu.cn (X. Liu).

0022-328X/$ - see front matter © 2009 Elsevier B.V. All rights reserved.
doi:10.1016/j.jorganchem.2009.12.007

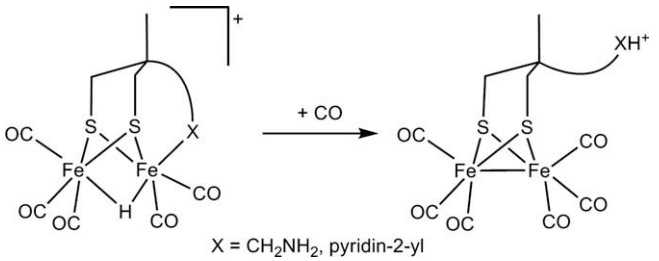

Scheme 1. Conversion of the bridging hydride (left) to the protonated hexacarbonyl complex (right).

to allow such detection. More interestingly, the latter hydride did not convert into diiron hexacarbonyl complex as those shown in Scheme 1. It would be pertinent to assume that the basicity of the bound internal base in both Brønsted–Lowry and Lewis acid–base concepts is associated with formation of the protonated diiron hexacarbonyl complexes as well as this hydride chemistry. But it is not clear how the basicity of the bound internal base correlates to the formation of the protonated diiron hexacarbonyl complexes and the stability of the bridging hydrides.

Recently, re-examination of the reaction which afforded the pyridine-containing diiron pentacarbonyl complex **C** [36] led to the isolation of another diiron pentacarbonyl complex **A**, which is equivalent to the product of partial hydrogenation of the pyridine ring in complex **C**, that is, partial hydrogenation of pyridine-2-yl produced 4*H*-1, 2, 5, 6-pyridin-2-yl. Protonation of this complex gave a rather stable μ-hydride as suggested by its infrared spectroscopy and NMR resonance. With our previously reported μ-hydride chemistry in mind [36], we were prompted to further explore how the stability of these hydrides was dictated and how they converted into protonated diiron hexacarbonyl complexes.

Herein, we report the isolation, characterisation, and protonation of complex **A**. By combining spectroscopic investigations and DFT calculations, correlation of the stability of the hydride of this complex and analogues previously reported [36], to the basicity of their internal bases was explored. In the light of DFT calculations, possible mechanisms for the conversion from the bridging hydrides to the protonated diiron hexacarbonyl complexes were also proposed.

2. Material and methods

2.1. General procedures

All reactions and operations were carried out under argon atmosphere with standard Schlenk techniques. Solvents were dried prior to use according to standard method. The preparation of the tridentate ligand, 2-methyl-2-(pyridin-2-yl) propane-1,3-dithiol (**H_2L′**) followed general procedures with minor modification [38]. $Fe_3(CO)_{12}$ was purchased from Sigma Aldrich and $HBF_4{\cdot}Et_2O$ from Alfa Aesar. All chemicals were used as received unless otherwise stated.

FTIR spectra were recorded on Scimitar 2000 (Varian) by using a cell with a spacer of 0.1 mm or KBr pellets. NMR spectra were measured on Bruker AVANCE III (400 MHz) with tetramethylsilane as internal standard. Elemental analyses were performed on a Heraeus CHN–O-Rapid or Elementar Vario MICRO elemental analyzer (Nanjing University).

2.2. Crystal structure analysis

Crystallographic data collection of complex **A** was carried out in the same manner as described elsewhere [39]. Its structure was solved by direct method using SHELXS-97 program [40] and refined on F^2 with XSHELL6.3.1. All non-hydrogen atoms were modelled anisotropically. All hydrogen atoms were positioned geometrically and treated as riding on their parent atoms with C–H distances at 0.93, 0.96, and 0.97 Å for alkenyl, methyl, methylene, and tertiary C–H, respectively, and with $U_{iso}(H) = 1.5\ U_{eq}(C)$ for methyl group but $U_{iso}(H) = 1.2\ U_{eq}(C)$ for the rest of the H atoms.

2.3. DFT calculations

DFT, as implemented in TURBOMOLE 5.7 [41,42], has been employed for determining all the stationary points, *i.e.* intermediates, and transition state structures, of the potential energy hypersurface associated with the reaction coordinate investigated. Functional adopted was the pure B-P86 [43,44] along with a triple-ζ quality basis set, which is a well suited choice for theoretical investigations of the diiron sub-unit of the [FeFe]-hydrogenase and its synthetic analogues [45–47]. Resolution of the Identity (RI) density fitting procedure [48] has allowed to shorten computing time by approximating the two-electron-four-centre integrals (necessary for determination of the Coulomb repulsions) with less computationally demanding three-centre integrals. Second derivatives of the DFT energy with respect to the nuclear positions (potential energy curvature) have also been analytically resolved in order to determine the true nature of all the stationary points located (*i.e.*, minima: all positive eigenvalues of the Hessian matrix; first-order saddle points or transition structure: all positive eigenvalues of the Hessian matrix but one negative eigenvalue associated to the molecular vibration leading to the reactive event). Algorithm employed to search for transient state structure is a pseudo-Newton–Raphson method, implemented with the TRIM [49] procedure and which entails an "eigen-vector-following" move along the PES in the region of the first-order saddle point. Such method performs extremely well only if a "good" guess of the true transition structure is used for the quest. Such good guess is located by freezing all those molecular degrees of freedom forming the reaction step, *i.e.* those bond lengths, angles or torsions which change most during the reaction event. Solvent corrections have been added, when necessary, to data calculated in gas phase. Dielectric constant value, employed for COSMO [50] modelling of polarisation effects deriving from solvent inclusion is 9.1, which correspond to dichloromethane at standard T values.

2.4. Synthesis

2.4.1. $[Fe_2(\mu\text{-}SCH_2)_2C(CH_3)(2\text{-}C_5H_8N)(CO)_5]$, **A**

To a solution of $Fe_3(CO)_{12}$ (0.216 g, 0.429 mmol) in dry toluene (5 ml) was added a solution of the tridentate ligand **H_2L′** (0.079 g, 0.40 mmol) in toluene (10 ml) under Ar atmosphere. The mixture was stirred at 110 °C for 4 h until the ligand was completely reacted as indicated by TLC. Removal of the solvent under reduced pressure produced a solid in dark colour which was purified with flash chromatography (eluent:ethyl acetate:hexanes = 1:4). Complex **A** (25 mg, 14%) was collected first and then the previously reported complex **C** (63 mg, 35%) [36]. Removal of the solvents yielded a brown solid. Crystals suitable for X-ray single crystal diffraction analysis was produced by layering hexanes onto its solution in dichloromethane. FTIR (CH_2Cl_2): 2047.9, 1975.2, 1909.2 cm^{-1}. ^1H NMR ($CDCl_3$): 0.82 (s, 3H, $-CH_3$), 1.385 (d, J = 13.8 Hz, 1H, –NH), 1.84 (d, J = 14.4 Hz, 1H, NC–CH_aH_b), 2.05 (d, J = 17.0 Hz, 1H, NC–CH_aH_b), 2.55 (q, 2H, $-NCH_2$), 2.98 (s, 2H, $-SCH_2$), 3.19 (s, 2H, $-SCH_2$), 4.40 (s, 1H, –NCH), 5.31 (d, J = 10.0 Hz, 1H, $-CH_a{=}CH_b$), 6.02 (s, 1H, $-CH_a{=}CH_b$). Microanalysis, calc. (found) for $C_{14}H_{15}Fe_2S_2NO_5$ (FW = 452.1): C, 37.19 (37.10); H, 3.12 (3.28); N, 3.10 (3.22)%.

*2.4.2. $[Fe_2(\mu\text{-}H)(\mu\text{-}SCH_2)_2C(CH_3)(2\text{-}C_5H_8N(CO)_5)]BF_4$, **AH$^+$***

To a solution of complex **A** (27 mg, 0.06 mmol) in toluene (10 ml) at −78 °C was added a large excess of $HBF_4{\cdot}Et_2O$ (295 μl, 35 eq.) under Ar. With a colour change from brown to dark red, a red oily liquid settled at the bottom of the reaction vessel. The liquid was washed with toluene after the solvent was removed by transferring through a canula. The preliminarily purified crude liquid was re-dissolved in a minimum dichloromethane and then was hexanes added to crush out the product, which was repeated once to produce the hydride, **AH$^+$** contaminated with minimum remaining acid. The liquid was dried in vacuum for a few hours. FTIR (CH_2Cl_2): 2109.0, 2057.5, 2008.9 cm^{-1}. ^1H NMR (CD_2Cl_2): −24.26 (s, 1H, μ-hydride), 1.15 (s, 3H, $-CH_3$), 1.84 (d, J = 14.60 Hz, 1H, –NH), 2.32 (d, J = 16.0 Hz, 1H, NC–CH_aH_b), 2.80 (d, J = 14.2 Hz, 1H, NC–CH_aH_b), 2.90 (d, J = 15.6 Hz, 1H, $-NCH_aH_b$), 3.17 (s, 1H, $-NCH_aH_b$), 3.37 (s, 2H, $-SCH_2$), 3.48 (s, 2H, $-SCH_2$), 5.25 (s, 1H, –NCH), 5.43 (d, J = 9.9 Hz, 1H, $-CH_a{=}CH_b$), 6.08 (s, 1H, $-CH_a{=}CH_b$).

*2.4.3. $[Fe_2(\mu\text{-}SCH_2)_2C(CH_3)(2\text{-}C_5H_8NH)(CO)_6]BF_4$, **ACOH$^+$***

To a solution of complex **A** (27 mg, 0.06 mmol) in acetonitrile (5 ml) saturated with CO was added $HBF_4{\cdot}Et_2O$ (53%, 12.7 μl, 0.09 mmol) at room temperature under stirring. Upon the addition, the brown solution instantly changed to light orange. An orange solid was produced by layering ethyl ether onto a solution of the complex in acetonitrile, which was collected by filtration and dried in vacuum. FTIR (CH_2Cl_2): 2077.8, 2038.3, 2007.4, 1975.1 cm^{-1}. ^1H NMR (CD_3CN): 1.09 (s, 3H, $-CH_3$), 2.17 (d, J = 6.51 Hz, 1H, NC–CH_aH_b), 2.21, (d, J = 6.4 Hz, NC–CH_aH_b), 2.35 (d, J = 13.8 Hz, 1H, $-NCH_aH_b$), 2.44 (d, J = 13.8 Hz, 1H, $-NCH_aH_b$), 3.14 (m, 2H, $-SCH_2$), 3.44 (q, 2H, $-SCH_2$), 3.86 (d, J = 13.8 Hz, 1H, –NCH), 5.59 (d, J = 10.7 Hz, 1H, $-CH_a{=}CH_b$), 6.13 (m, 1H, $-CH_a{=}CH_b$), 6.35 (br, s, 1H, $-NH_aH_b$), 6.84 (br, s, 1H, $-NH_aH_b$).

*2.4.4. Conversion of **AH$^+$** into **ACOH$^+$** under CO atmosphere*

Hydride **AH$^+$** which was prepared and stored in a Schlenk tube at low temperature prior to use was dissolved in dichloromethane. The solution which contains unremoved acid from its preparation was purged with CO for a few hours for saturation and stirred at 298 K. The initial concentration of the hydride was arbitrary due to difficulty in removing the unreacted acid from its preparation (Section 2.4.2). The conversion reaction was followed by using infrared spectroscopy.

3. Results and discussion

3.1. Synthesis and structural analysis

The reaction of the tripodal ligand, 2-methyl-2-(pyridin-2-yl)propane-1,3-dithiol (**H_2L'**) [36], with tri-iron dodecacarbonyl in dry toluene produced a diiron pentacarbonyl complex (**C**) by following a general procedure [11]. Further examination of the reaction led to the isolation of another diiron pentacarbonyl complex **A** in *ca.* 14% yield, Scheme 2. Interestingly, complex **A** looks structurally the result of partial hydrogenation of the pyridinyl ring in complex **C**. But during the reaction, how the pyridin-2-yl group was converted into 4*H*-1,2,5,6-pyridin-2-yl, that is, how the original ligand **H_2L'** "evolved" into 2-methyl-2-(1,2,5,6-tetrahydropyridin-2-yl)propane-1,3-dithiol, is not clear yet. However, it has been well known that pyridine ring can be partially hydrogenated by sodium tetrahydroborate [51–52]. In this case, the partial reduction of the pyridinyl ring is, presumably, associated with the reductive deprotonation of the dithiol of ligand **H_2L'** in its reaction with tri-iron dodecacarbonyl, in which perhaps a hydride or hydrogen might be involved.

Complex **A** was crystallographically analysed. Its crystallographic details is summarised in Table 1. The structural view of this complex alongside with selected bond lengths and angles is shown in Fig. 1. Structurally, complex **A** is essentially identical to other diiron analogues reported [11,36–37].

In dichloromethane solution, this complex shows two sharp absorption bands at 2047.9 and 1975.2 cm^{-1} plus a much weaker one at 1909.2 cm^{-1} as shown in Fig. 2, which exhibits an infrared spectral envelope of characteristic for all diiron pentacarbonyl complexes [5,8,15,37,53]. Compared to the amine- (**B** as designated in Scheme 2) and pyridine-containing (**C**, Scheme 2) analogues reported previously [36], its absorption bands shifted down to lower frequencies by approximately 2 and 4 cm^{-1} by average, respectively, which indicates better electron-donating ability of the secondary amine in complex **A**. In the three complexes, **A**, **B**, and **C**, the organic moieties possess a secondary, primary amines, and pyridin-2-yl derivative, respectively. Typical pK_b values for bases of these types are 2.93 ± 0.32, 3.42 ± 0.19, and 8.10 ± 0.17, respectively [54–57]. By further considering the model complex reported [8], $[Fe_2(\mu\text{-}SCH_2)_2CMe(CH_2SMe)(CO)_5]$ (**D**, Scheme 2), whose thioether has much weaker basicity (in one example, the pK_b value of such a thioether was estimated at 20.8) [58,59], a linear correlation between the averages of the three infrared absorption bands of the diiron pentacarbonyl complexes and the pK_b values of the bases

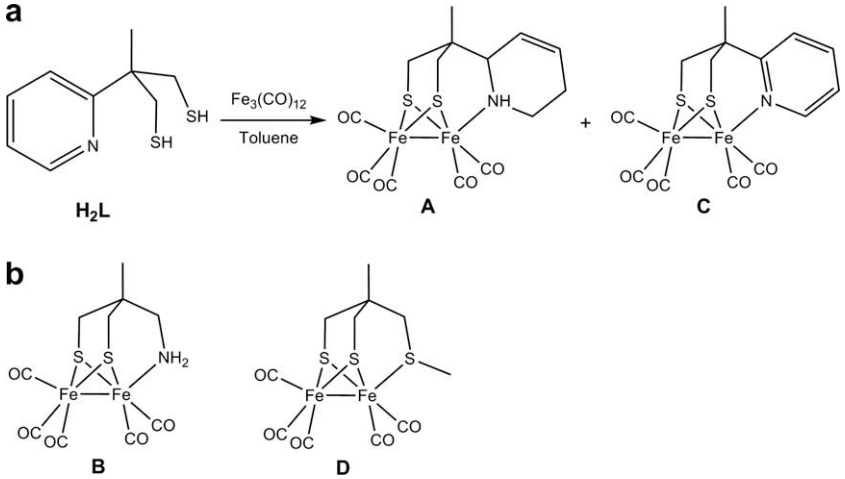

Scheme 2. (a) Synthesis of the diiron pentacarbonyl complexes **A** and **C**, and (b) the structural presentations of the other two complexes **B** and **D**.

Table 1
Crystallographic data and structure refinement for complex **A** (CCDC 742571).

Empirical formula	$C_{14}H_{14}Fe_2NO_5S_2$
Formula weight	452.10
Temperature (K)	293(2)
Wavelength (Å)	0.71073
Crystal system	Monoclinic
Space group	*P*21/*c*
Unit cell dimensions	
a (Å)	9.3887(13)
b (Å)	17.394(2)
c (Å)	12.3982(13)
α (°)	90
β (°)	117.954(8)
γ (°)	90
Volume (Å^3)	1788.5(4)
Z	4
D_{calc} (Mg/m^3)	1.686
Absorption coefficient (mm^{-1})	1.878
F(0 0 0)	916.0
Crystal size (mm)	0.576 × 0.141 × 0.073
Theta range for data collection	2.20–26.00
Index ranges	
$-11 \leqslant h \leqslant 11$	
$-21 \leqslant k \leqslant 21$	
$-14 \leqslant l \leqslant 15$	
Reflections collected	11440
Independent reflections	3472 [$R_{(int)}$ = 0.0266]
Completeness to theta = 26.00	98.5%
Absorption correction	–
Refinement method	Full-matrix least-squares on F^2
Data/restraints/parameters	3472/0/218
Goodness-of-fit on F^2	0.989
Final *R* indices [$I > 2\sigma(I)$]	R_1 = 0.0295, wR_2 = 0.0848
R indices (all data)	R_1 = 0.0419, wR_2 = 0.0903
Largest diff. peak and hole (e Å^{-3})	0.578 and −0.252

analogous to the internal bases in the corresponding complexes was observed, Fig. 3. This relationship demonstrates the electronic effect of the bound internal base on the CO stretching frequencies.

3.2. Protonation of complex *A* and conversion of its bridging hydride *AH*$^+$ into complex *ACOH*$^+$

Protonation of complex **A** under Ar atmosphere at room temperature produced a mixture of bridging hydride **AH**$^+$ and protonated dinuclear hexacarbonyl complex **ACOH**$^+$, which were confirmed by infrared and ^{1}H NMR spectroscopies. Lowering operation temperature (−78 °C) could essentially suppress forming **ACOH**$^+$ and the bridging hydride (**AH**$^+$) was nearly quantitatively generated, Fig. 2. On the other hand, complex **ACOH**$^+$ could form quantitatively under CO atmosphere. In spite of the correlation of the basicities of the analogous bases to the infrared absorption bands of those diiron complexes (Fig. 3), the formation of the bridging hydrides **AH**$^+$, and the other three hydrides (**BH**$^+$, **DH**$^+$, and **CH**$^+$) [36], upon protonation of their parent complexes does not follow this trend. In fact, no bridging hydride was detectable for complex **C**, and no hexacarbonyl complex **DCOH**$^+$ for **D** at room temperature under Ar atmosphere, whereas for complex **B**, which is similar to complex **A**, a mixture of protonated hexacarbonyl complex **BCOH**$^+$ and bridging hydride **BH**$^+$ formed under the same conditions. Apparently, there is no simple correlation between the formation of these hydrides and the basicities of the corresponding bound internal bases. It is noteworthy that as **BH**$^+$ [36], the bridging hydride **AH**$^+$ also converts slowly into its hexacarbonyl complex at room temperature and this conversion occurred in various solvents (for example, dichloromethane, THF, and acetonitrile). It is particularly important to note that the conversion of the hydride **AH**$^+$ was very slow even under CO atmosphere at room

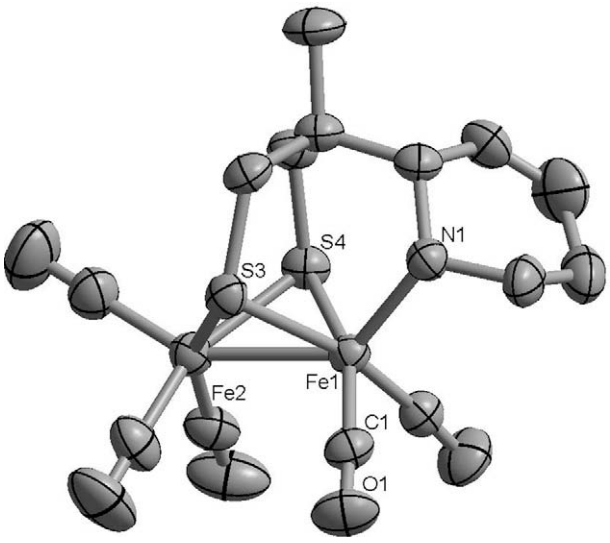

Fig. 1. Structural view of complex **A** (the ellipsoids thermal probability are drawn at 50% level and hydrogen atoms are omitted for clarity); selected bond lengths (Å) and angles (°): Fe1–Fe2 = 2.514, Fe1–N1 = 2.063, Fe1–S1 = 2.264, Fe2–S1 = 2.262, Fe1–S2 = 2.259, Fe2–S2 = 2.261, Fe1–C10 = 1.767, C10–O1 = 1.143, ∠Fe2–Fe1–C10 = 108.7, ∠N1–Fe1–S1 = 99.92, ∠S1–Fe1–S2 = 86.15, and ∠Fe1–S1–Fe2 = 67.47.

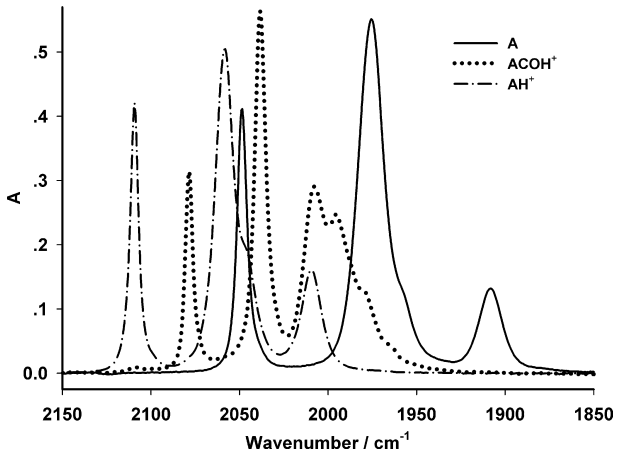

Fig. 2. Infrared spectra of complexes **A**, its bridging hydride **AH**$^+$ and the protonated hexacarbonyl complex **ACOH**$^+$ in dichloromethane.

temperature, Fig. 4. As reported previously, [36] there are two pathways for the formation of the protonated dinuclear hexacarbonyl complexes, one of which is *via* the bridging hydride intermediate. Since both pathways could lead to the protonated hexacarbonyl complex, it is mechanistically interesting to find out whether the variation in the hydride formation is associated to the stability of the hydride or to adopting different pathways. One way to discriminate this chemistry is to examine the stability of the aforementioned hydrides with various internal bases and to explore how the basicity of the internal base plays a role in the stability of a hydride and its subsequent conversion.

To this end, theoretic calculations were performed. It is worth anticipating that formation of terminal bound hydrides has not been taken into account, mainly because no related spectroscopic evidence has been revealed for these derivatives, neither at low temperature conditions. Therefore, the entire DFT part has focused onto formation of bridging hydrides and their subsequent evolution to protonated hexacarbonyl products. In the calculations, the acid ($HBF_4{\cdot}Et_2O$) and solvent (dichloromethane) used in our experimental investigations were taken into account. For these forma-

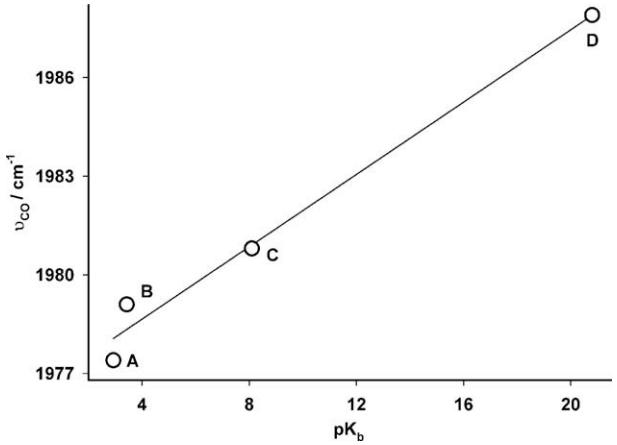

Fig. 3. Correlation of the averages of the three infrared absorption bands (taken in dichloromethane) for the diiron pentacarbonyl complexes (**A**, **B**, **C**, and **D**) to the pK_b values of analogous bases (primary amine, secondary amine, and pyridinyl derivatives) comparable to the organic moieties in these complexes (1976.5 + 0.55 pK_b, R = 0.99).

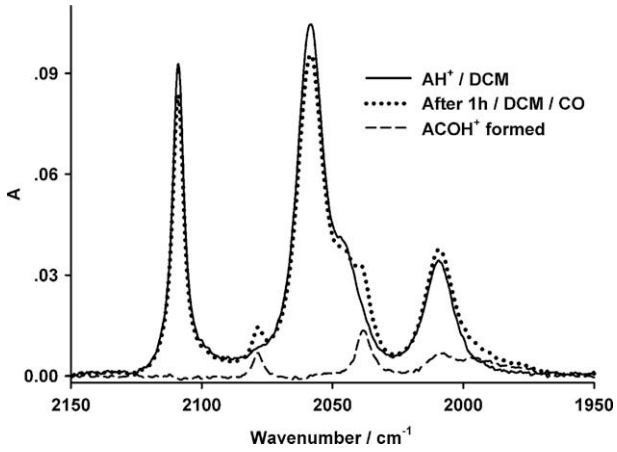

Fig. 4. Conversion of **AH$^+$** into **ACOH$^+$** in dichloromethane under CO atmosphere at 298 K.

tion reactions of these bridging hydrides, **AH$^+$**, **BH$^+$**, **CH$^+$**, and **DH$^+$**, Gibbs free energy, $\Delta G°$, were −20.2, −21.9, −15.2, and −10.6 kcal mol^{-1}, respectively. These data do show that formation of the bridging hydrides for all these complexes is thermodynamically favoured. But the formation of these bridging hydrides experimentally observed upon protonation does not correlate well to these data.

To further address the thermodynamics related to the stabilities of the bridging hydrides, we have also computed $\Delta G°$ for the protonating reactions of the binuclear complexes **A**, **B**, **C**, and **D** under CO atmosphere, Scheme 3 (**b**). It turned out that along the vector from **A** to **D**, the $\Delta G°$ values are -33.9, -24.0, -25.2 and 1.0 kcal mol^{-1}, respectively. Fundamentals of chemical reaction equilibrium tells that the conversion from bridging hydride to the protonated hexacarbonyl complex, Scheme 3 (**c**), is the subtraction result of (**b**–**a**). Hence, the $\Delta G°$ values for the conversion are easily derived from the subtraction, that is, −13.7, −2.1, −10.0, and 11.6 kcal mol^{-1}, respectively. The clear-cut boundary in these data between the N-containing complexes and the thioether-based analogue instantly explains why the latter complex has the most stable hydride in solution. But notably, the trend of the data for the N-containing complexes cannot appropriately correlate to the formation chemistry of these hydrides. This implies that the conversion of these bridging hydrides is not simply governed by the basicity.

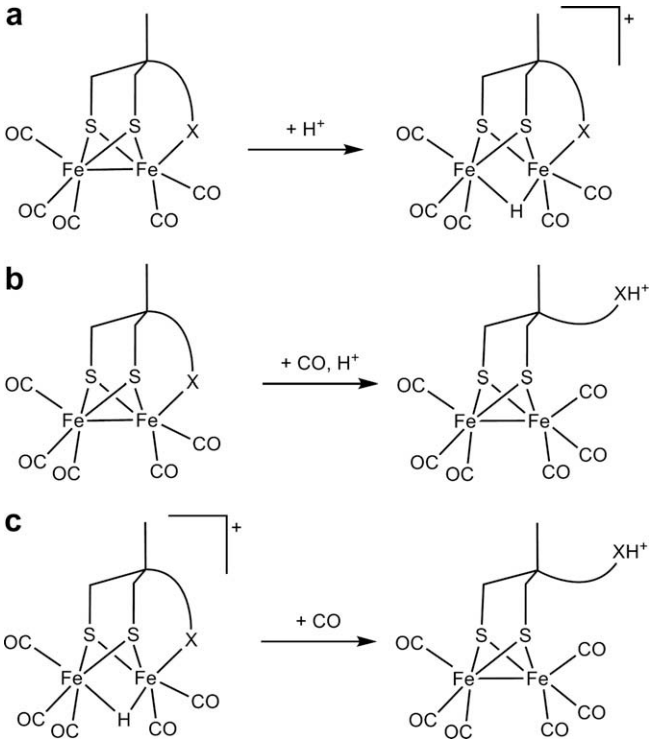

Scheme 3. Reactions involving the formation of bridging hydrides and protonated diiron hexacarbonyl complexes (X = CH_2NH_2, pyridine-2-yl, and 4*H*-1, 2, 5, 6-pyridin-2-yl).

*3.3. Possible pathways for transformation of the bridging hydride complex **AH$^+$** into the protonated diiron hexacarbonyl complex **ACOH$^+$***

As mentioned above, the formation of the hydrides upon protonating their parent complexes, **A**, **B**, **C**, and **D**, varies greatly from one to another. For the complex **D**, the protonation occurs only at the metal–metal bond to give a stable hydride **DH$^+$** while the pyridine-containing analogue **C** gave no detectable hydride upon protonation under the same conditions [36]. For complex **A**, the protonation could stop at the stage of hydride, which allowed its isolation and further characterisation. To fully elucidate the hydride formation, stability, and subsequent conversion, it is necessary to examine theoretically how the conversion proceeds. Such investigations would be beneficial to designing novel model complexes possessing protonable groups which may play a role in catalytic reduction of proton.

To shed some light on the conversion mechanism and highlight possible differences depending on the nature of the pendant ligands, we have used DFT calculations to search for intermediate species and transition states assuming an intramolecular reaction pathway. This last assumption is motivated in the light of experimental data (see above) which show no solvent effect onto proton migration process, thus allowing us to exclude quite confidently possible mechanisms entailing the activity of acid–base/intermolecular shuttles of H$^+$. Also, two other preliminary issues hold true in a general sense:

(i) No intermediate has been found for all the four species investigated, which features a terminal hydride being coordinated in an axial fashion. This last is in principle conceivable to exist transiently before H$^+$ leaves Fe coordination

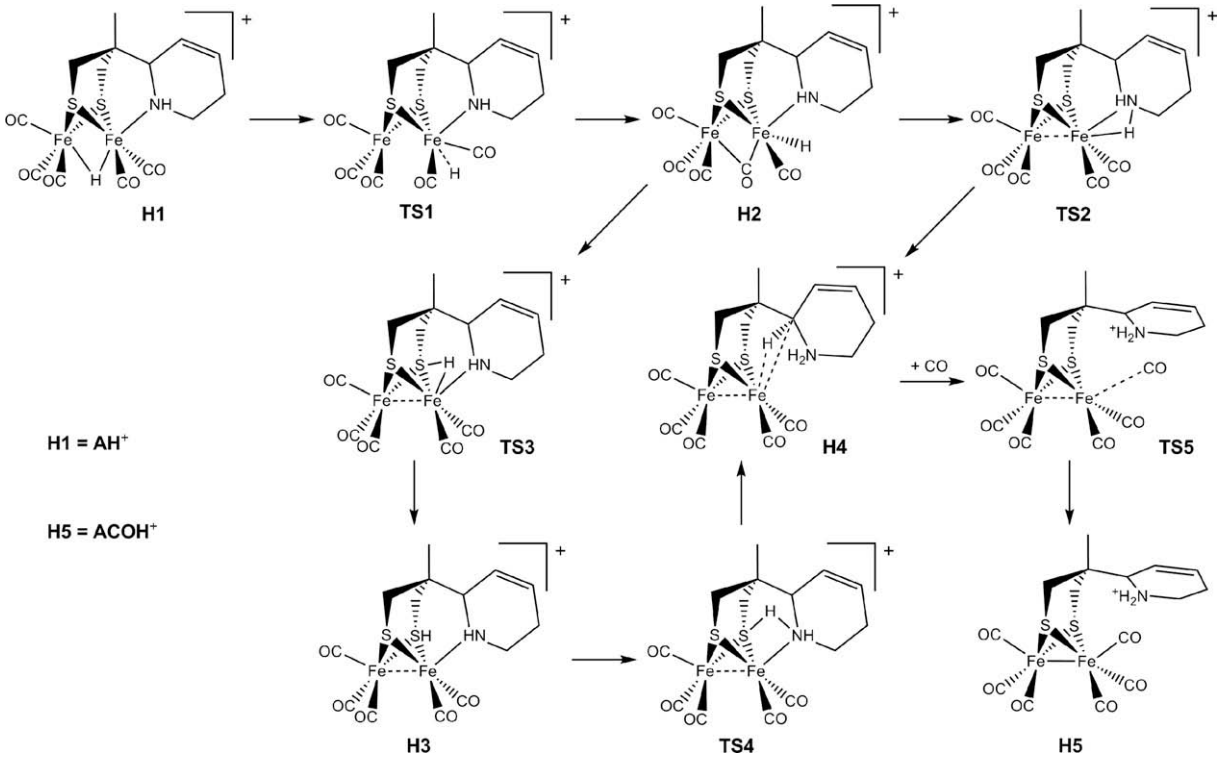

Scheme 4. Two pathways generated from DFT calculations for the conversion from the bridging hydride (**AH**$^+$) to the protonated diiron hexacarbonyl complex (**ACOH**$^+$).

sphere to attack the N-containing pendant. However, it is noteworthy that such a pseudo-axial coordination mode of the hydride ligand is actually encountered at transition state level (**TS2**; see below in Scheme 4 and Fig. 5)

(ii) No other intramolecular route except the two illustrated in the following has been detected for proton migration from Fe–Fe bond to N atom. Indeed, both pathways can be depicted as intramolecular reductive eliminations, in which the bridging hydride releases two electrons to Fe and concomitantly migrates to either N atom directly or *via* S atoms of dithiolate linker. In the second case, the reductive elimination event occurs when H^+ binds to the S lone-pair. All these considerations mean that no dissociative pathway has been located, namely, in which the N–Fe (or S–Fe) bond breaks independently from H^+ transfer. Computational results show that actually no penta-coordinated stable structure is detectable which features the N- or S- pendant dissociated from the iron ion, when the hydride is still coordinated to the iron itself.

In the calculations, the bridging hydrides, **AH**$^+$, **BH**$^+$, **CH**$^+$, and **DH**$^+$, were assumed as the precursors for the conversion. Computa-

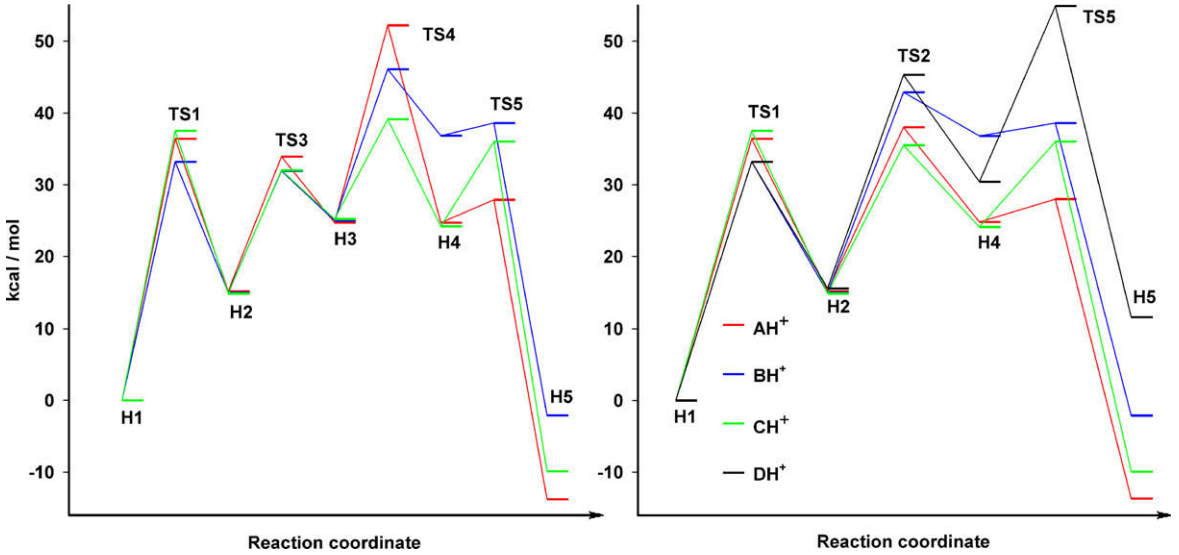

Fig. 5. Changes in energy levels in pathway **M1** (left panel), in which one of the thiolate relays the proton, and in pathway **M2** (right panel) for the transformation from the bridging hydrides **H1** (**AH**$^+$, **BH**$^+$, **CH**$^+$, and **DH**$^+$) to **H5** (**ACOH**$^+$, **BCOH**$^+$, **CCOH**$^+$, and **DCOH**$^+$). Please note that the formation of **DCOH**$^+$ is not applicable in the pathway **M1**.

tional results show that the four hydrides fall mechanistically into two categories. The three N-containing hydrides take highly similar courses in the conversion into their protonated hexacarbonyl complexes. Pathways for the conversion of **AH**$^+$ into **ACOH**$^+$ are delineated in Scheme 4. As shown in Scheme 4, the possibility of CO binding directly to the hydride might be excluded by means of simple considerations, such as the more feasible displacement from Fe of an agostic interaction (**H4**, Scheme 4) with respect to a lone-pair of a N- or S-containing ligand. Nevertheless, the energy barrier for CO entry directly onto bridging hydride species has been computed in the case of complex **B** and it turned out to be over 40 kcal mol^{-1}, which further strengthens our argument that CO must bind to the dinuclear complex at subsequent stages rather than bind directly to the hydride.

Scheme 4 depicts possible converting pathways for hydride **AH**$^+$. There are two feasible pathways for the conversion. In one pathway (**M1**), one of the bridging thiolate is used as relaying site *via* two transient states, **TS3** and **TS4**. **TS3** is a three-centred structure in which the nature of the hydride is more protic than hydric. Species **H4** could also be achieved through the other pathway (**M2**) *via* **TS2**. The variations in energy level for those species and transient states along reaction coordinate are shown in Fig. 5. Possible converting pathways for the other hydrides conversions are shown in Scheme S1, S2, and S3, respectively.

Performing the same calculations on the hydride **DH**$^+$ led to a rather different scenario, in which pathway **M1** simply cannot hold valid. All the energies for each step of the two pathways, **M1** and **M2**, are tabulated in Table 2. As indicated by Fig. 5 and the data shown in Table 2, there are some straightforward correlations between the theoretic aspects and experimental observations related to the conversion from the bridging hydride into the protonated hexacarbonyl complexes. The conversion is exoergonic for all the hydrides except that of the thioether-based analogue (**DH**$^+$). The Gibbs free energy for the conversion is −13.7, −2.1, −10.0, and 11.6 kcal mol^{-1} for **AH**$^+$, **BH**$^+$, **CH**$^+$, and **DH**$^+$, respectively. This is in agreement with the experimental observation that the thioether analogue did not form the protonated dinuclear hexacarbonyl complex upon protonation as discussed earlier.

The energy barrier for the step from **H4** to **TS5**, in which the exogenic CO comes in, is satisfactorily correlated to the basicity of the bound internal base. For the pyridine- and thioether-containing analogues (**CH**$^+$ and **DH**$^+$) which are less basic, much larger uphill energy change (24.5 and 11.8 kcal mol^{-1}, respectively) is observed compared to those (<3.2 kcal mol^{-1}) for the other two N-based analogues (**AH**$^+$ and **BH**$^+$). The energetic for this process is entirely consistent with that stronger protophilicity would facilitate the cleavage of the bound internal bases by protonation. But it is necessary to note that in the concept of Lewis acid–base, the thioether is not a weak base. This is rationalised by that species **H4** is not like the others featuring agostic interaction with nearby C–H bond in the hypothetic conversion of this thioether analogue, which implies that the lone-pair on the S atom is a better electron source to satisfy the demand of the proximal Fe in electron. It is noteworthy that hydride **CH**$^+$ could have comparable stability to that of the thioether-based analogue, but experimental observation reported previously [36] is entirely contrary to this theoretic expectation. We attribute this to the hemi-lability of the Fe(I)–N(Py) bond (*vide infra*).

For the three N-containing hydrides (**AH**$^+$, **BH**$^+$, and **CH**$^+$), the conversion pathway **M1** is energetically more favoured compared to pathway **M2**. As shown in Table 2, the energetic barrier for the step from **H3** to **TS4** correlates well with the basicity of the internal base, that is, the hydride **AH**$^+$ with the most basic internal base possessing the highest energy level whereas for the hydride **CH**$^+$, this energetic barrier is the lowest. This is highly in line with the experimental observation that the hydride **AH**$^+$ has the longest life-time compared to those of the other two. The proton acidity of HS-{Fe_2S} in **H3**, governs the formation of the **TS4** whereas this acidity is, in turn, affected by the basicity of the internal base which binds to the diiron centre. It is well known that acidity of a substituted phenol is enhanced by electron-withdrawing groups and weakened by substituents with electron-donating nature.[60] By analogy, we would expect that HS-{Fe_2S} of **H3** is the least acidic for **AH**$^+$, which disfavours forming the transient state **TS4**.

As revealed by Fig. 5 and the data shown in Table 2, both pathways possess two steps showing significant variations in kinetic barriers, which may be the key steps to differentiate the stability of these hydrides. For both mechanisms, step **H4** → **TS5** is one of the two key steps. For pathway **M2**, the other step is **H2** → **TS2** whereas for pathway **M1**, it is the step, **H3** → **TS4**. By analysing the calculated energy barriers of these key steps and experimental observations, pathway **M1** is strongly favoured for the conversion of these hydrides into corresponding protonated diiron hexacarbonyl complexes except the thioether analogue **DH**$^+$ for which no valid pathway could be located for **H3** → **TS4** to proceed. The energy profiles for this key step are in good agreement with the protonating behaviours observed experimentally (Section 3.2). In this pathway (**M1**), the role of the bound internal base played in the conversion is entirely opposite to each other. In the step, **H3** → **TS4**, strong basicity is unfavourable whereas in the other step (**H4** → **TS5**), strong basicity is beneficial to the conversion by facilitating the cleavage of the iron bound internal through protonation. Only the conversion of the hydride **CH**$^+$ is seemingly at odds with the calculated results in the step, **H4** → **TS5**. This can probably attributed to the hemi-lability of the Fe–N (pyrdinyl) coordination. As reported previously [36], the parent complex **C** is the only one which underwent CO-substitution reaction under CO atmosphere. For the thioether analogue **D**, the conversion is strongly disfavoured due to the poor protophilicity of the thioether in this complex.

4. Conclusions

A diiron model complex bearing a bound internal base resulting from unusual hydrogenation of pyridinyl group was fully charac-

Table 2
Energetics (kcal mol^{-1}) for each step involving the transformation from **H1** (**AH**$^+$, **BH**$^+$, **CH**$^+$, **DH**$^+$) to **H5** (**ACOH**$^+$, **BCOH**$^+$, **CCOH**$^+$, **DCOH**$^+$).

Hydride pathway	AH+		BH+		CH+		DH+	
	M1	M2	M1	M2	M1	M2	M1	M2
H1 → TS1	36.4	36.4	33.2	33.2	37.5	37.5	33.2	33.2
TS1 → H2	−21.2	−21.2	−18.2	−18.2	−22.6	−22.6	−17.6	−17.6
H2 → TS3 (TS2)	18.7	22.8	16.9	27.9	17.1	20.6	15.3	29.7
TS3 → H3	−9.2	n/a	−6.9	n/a	−6.8	n/a	−7.8	n/a
H3 → TS4	27.5	n/a	21.1	n/a	13.9	n/a	n/a	n/a
TS4 (TS2) → H4	−27.5	−13.2	−9.3	−6.1	−14.9	−11.4	n/a	−14.9
H4 → TS5	3.2	3.2	1.8	1.8	11.8	11.8	n/a	24.5
TS5 → H5	−41.7	−41.7	−40.7	−40.7	−45.9	−45.9	n/a	−43.3

terised. Its protonating reaction produced a stable bridging hydride which allowed its identification by NMR spectroscopy. While the infrared absorption bands of this diiron pentacarbonyl complex and other analogues possess linear correlation with the pK_b values of bases analogous to those internal bases in the investigated model complexes, there is no simple correlation of the formation of the hydrides to the basicity of the internal base upon protonation. Theoretical analysis revealed that all the hydrides are reasonably stable. This revelation suggests that the formation of the protonated dinuclear hexacarbonyl complexes from the examined diiron pentacarbonyl complexes is mainly through other pathway rather than that *via* the bridging hydride. But the conversion of the hydride into the protonated dinuclear hexacarbonyl complex *via* an intramolecular migration mechanism is thermodynamically possible except for **DH$^+$**. In the conversion, there are three factors governing how feasible it is, which are basicity, protophilicity, and hemi-lability of the Fe–N bond. Delicate balance of the effects of these controlling factors exerted in the two key steps, **H3** → **TS4** and **H4** → **TS5**, determines the stability of these hydrides or the feasibility of their conversions.

Two pathways, **M1** and **M2**, for the conversion were derived from the theoretical calculations. Overall considerations suggest that pathway **M1** is most likely. It is noteworthy that the bridging thiolate is a favourable site for transferring hydride/proton in this pathway. The possibility of the thiolate as a potential proton transferring site was also suggested by theoretical investigations of the [FeFe]-hydrogenase [61–63].

Acknowledgements

We thank the Natural Science Foundation of China (Grant No. 20871064), Ministry of Science and Technology of China (973 program, 2009CB220009), and Centre of Analysis and Testing at Nanchang University for supporting this work.

Appendix A. Supplementary material

Supplementary data associated with this article can be found, in the online version, at doi:10.1016/j.jorganchem.2009.12.007.

References

[1] J.W. Peters, W.N. Lanzilotta, B.J. Lemon, L.C. Seefeldt, X-ray crystal structure of the Fe-only hydrogenase (Cpl) from Clostridium pasteurianum to 1.8 angstrom resolution, Science 282 (5395) (1998) 1853–1858.
[2] Y. Nicolet, C. Piras, P. Legrand, C.E. Hatchikian, J.C. Fontecilla-Camps, *Desulfovibrio desulfuricans* iron hydrogenase: the structure shows unusual coordination to an active site Fe binuclear center, Struct. Fold. Des. 7 (1) (1999) 13–23.
[3] F. Gloaguen, J.D. Lawrence, M. Schmidt, S.R. Wilson, T.B. Rauchfuss, Synthetic and structural studies on [Fe-2(SR)(2)(CN)(*x*)(CO)(6 − *x*)](*x*−) as active site models for Fe-only hydrogenases, J. Am. Chem. Soc. 123 (50) (2001) 12518–12527.
[4] M. Razavet, A. Le Cloirec, S.C. Davies, D.L. Hughes, C.J. Pickett, X-Ray crystallographic analysis of D,L-[Fe-2{SCH_2CH–(CH_2OH)S}(CO)(6)] reveals a hydrogen-bonded cyclic hexamer with ordered optical centres, J. Chem. Soc., Dalton Trans. 24 (2001) 3551–3552.
[5] S.J. George, Z. Cui, M. Razavet, C.J. Pickett, The di-iron subsite of all-iron hydrogenase: mechanism of cyanation of a synthetic {$2Fe_3S$} – carbonyl assembly, Chem. Eur. J. 8 (17) (2002) 4037–4046.
[6] F. Gloaguen, J.D. Lawrence, T.B. Rauchfuss, M. Benard, M.M. Rohmer, Bimetallic carbonyl thiolates as functional models for Fe-only hydrogenases, Inorg. Chem. 41 (25) (2002) 6573–6582.
[7] D.J. Evans, C.J. Pickett, Chemistry and the hydrogenases, Chem. Soc. Rev. 32 (5) (2003) 268–275.
[8] M. Razavet, S.C. Davies, D.L. Hughes, J.E. Barclay, D.J. Evans, S.A. Fairhurst, X.M. Liu, C.J. Pickett, All-iron hydrogenase: synthesis, structure and properties of {$2Fe_3S$}-assemblies related to the di-iron sub-site of the H-cluster, Dalton Trans. 4 (2003) 586–595.
[9] S.J. Borg, T. Behrsing, S.P. Best, M. Razavet, X.M. Liu, C.J. Pickett, Electron transfer at a dithiolate-bridged diiron assembly: electrocatalytic hydrogen evolution, J. Am. Chem. Soc. 126 (51) (2004) 16988–16999.
[10] M.H. Cheah, S.J. Borg, M.I. Bondin, S.P. Best, Electrocatalytic proton reduction by phosphido-bridged diiron carbonyl compounds: distant relations to the H-cluster?, Inorg Chem. 43 (18) (2004) 5635–5644.
[11] X.M. Liu, S.K. Ibrahim, C. Tard, C.J. Pickett, Iron-only hydrogenase: synthetic, structural and reactivity studies of model compounds, Coord. Chem. Rev. 249 (15–16) (2005) 1641–1652.
[12] C. Tard, X.M. Liu, S.K. Ibrahim, M. Bruschi, L. De Gioia, S.C. Davies, X. Yang, L.S. Wang, G. Sawers, C.J. Pickett, Synthesis of the H-cluster framework of iron-only hydrogenase, Nature 433 (7026) (2005) 610–613.
[13] M.H. Cheah, C. Tard, S.J. Borg, X.M. Liu, S.K. Ibrahim, C.J. Pickett, S.P. Best, Modeling [Fe–Fe] hydrogenase: evidence for bridging carbonyl and distal iron coordination vacancy in an electrocatalytically competent proton reduction by an iron thiolate assembly that operates through Fe(0)–Fe(II) levels, J. Am. Chem. Soc. 129 (36) (2007) 11085–11092.
[14] S. Ezzaher, J.F. Capon, F. Gloaguen, F.Y. Petillon, P. Schollhammer, J. Talarmin, Electron-transfer-catalyzed rearrangement of unsymmetrically substituted diiron dithiolate complexes related to-the active site of the [FeFe]-hydrogenases, Inorg. Chem. 46 (23) (2007) 9863–9872.
[15] S.K. Ibrahim, X.M. Liu, C. Tard, C.J. Pickett, Electropolymeric materials incorporating subsite structures related to iron-only hydrogenase: active ester functionalised poly(pyrroles) for covalent binding of {$2Fe_3S$}-carbonyl/cyanide assemblies, Chem. Commun. 15 (2007) 1535–1537.
[16] A.K. Justice, G. Zampella, L. De Gioia, T.B. Rauchfuss, J.I. van der Vlugt, S.R. Wilson, Chelate control of diiron(I) dithiolates relevant to the [Fe–Fe]-hydrogenase active site, Inorg. Chem. 46 (5) (2007) 1655–1664.
[17] C. Mealli, T.B. Rauchfuss, Models for the hydrogenases put the focus where it should be-hydrogen, Angew. Chem., Int. Ed. 46 (47) (2007) 8942–8944.
[18] D. Morvan, J.F. Capon, F. Gloaguen, A. Le Goff, M. Marchivie, F. Michaud, P. Schollhammer, J. Talarmin, J.J. Yaouanc, R. Pichon, N. Kervarec, N-heterocyclic carbene ligands in nonsymmetric diiron models of hydrogenase active sites, Organometallics 26 (8) (2007) 2042–2052.
[19] L.C. Song, B.S. Yin, Y.L. Li, L.Q. Zhao, J.H. Ge, Z.Y. Yang, Q.M. Hu, Synthesis, structural characterization, and some properties of new N-functionally substituted diiron azadithiolate complexes as biomimetic models of iron-only hydrogenases, Organometallics 26 (2007) 4921–4929.
[20] S. Ezzaher, J.F. Capon, F. Gloaguen, N. Kervarec, F.Y. Petillon, R. Pichon, P. Schollhammer, J. Talarmin, Diiron chelate complexes relevant to the active site of the iron-only hydrogenase, C. R. Chim. 11 (8) (2008) 906–914.
[21] L.C. Song, C.G. Li, J. Gao, B.S. Yin, X. Luo, X.G. Zhang, H.L. Bao, Q.M. Hu, Synthesis, structure, and electrocatalysis of diiron C-functionalized propanedithiolate (PDT) complexes related to the active site of [FeFe]-hydrogenases, Inorg. Chem. 47 (11) (2008) 4545–4553.
[22] C. Tard, C.J. Pickett, Structural and functional analogues of the active sites of the [Fe]-, [NiFe]-, and [FeFe]-hydrogenases, Chem. Rev. 109 (6) (2009) 2245–2274.
[23] K.A. Vincent, A. Parkin, F.A. Armstrong, Investigating and exploiting the electrocatalytic properties of hydrogenases, Chem. Rev. 107 (10) (2007) 4366–4413.
[24] P.E.M. Siegbahn, J.W. Tye, M.B. Hall, Computational studies of [NiFe] and [FeFe] hydrogenases, Chem. Rev. 107 (10) (2007) 4414–4435.
[25] J.F. Capon, F. Gloaguen, F.Y. Petillon, P. Schollhammer, J. Talarmin, Electron and proton transfers at diiron dithiolate sites relevant to the catalysis of proton reduction by the [FeFe]-hydrogenases, Coord. Chem. Rev. 253 (9–10) (2009) 1476–1494.
[26] T. Liu, M.Y. Darensbourg, A mixed-valent, Fe(II)Fe(I), diiron complex reproduces the unique rotated state of the [FeFe]hydrogenase active site, J. Am. Chem. Soc. 129 (22) (2007) 7008–7009.
[27] X. Zhao, I.P. Georgakaki, M.L. Miller, R. Mejia-Rodriguez, C.-Y. Chiang, M.Y. Darensbourg, Catalysis of H_2/D_2 Scrambling and other H/D exchange processes by [Fe]-hydrogenase model complexes, Inorg. Chem. 41 (15) (2002) 3917–3928.
[28] J.L. Nehring, D.M. Heinekey, Dinuclear iron isonitrile complexes: models for the iron hydrogenase active site, Inorg. Chem. 42 (14) (2003) 4288–4292.
[29] T. Zhou, Y. Mo, A. Liu, Z. Zhou, K.R. Tsai, Enzymatic mechanism of Fe-only hydrogenase: density functional study on H−H Making/breaking at the diiron cluster with concerted proton and electron transfers, Inorg. Chem. 43 (3) (2004) 923–930.
[30] W.B. Dong, M. Wang, X.Y. Liu, K. Jin, G.H. Li, F.J. Wang, L.C. Sun, An insight into the protonation property of a diiron azadithiolate complex pertinent to the active site of Fe-only hydirogenases, Chem. Commun. 3 (2006) 305–307.
[31] L. Schwartz, G. Eilers, L. Eriksson, A. Gogoll, R. Lomoth, S. Ott, Iron hydrogenase active site mimic holding a proton and a hydride, Chem. Commun. 5 (2006) 520–522.
[32] F.I. Adam, G. Hogarth, I. Richards, Models of the iron-only hydrogenase: Reactions of $[Fe_2(CO)_6$([mu]-pdt)] with small bite-angle diphosphines yielding bridge and chelate diphosphine complexes $[Fe_2(CO)_4$(diphosphine)([mu]-pdt)], J. Organomet. Chem. 692 (18) (2007) 3957–3968.
[33] G. Eilers, L. Schwartz, M. Stein, G. Zampella, L. de Gioia, S. Ott, R. Lomoth, Ligand versus metal protonation of an iron hydrogenase active site mimic, Chem. Eur. J. 13 (25) (2007) 7075–7084.
[34] N. Wang, M. Wang, T.T. Zhang, P. Li, J.H. Liu, L.C. Sun, A proton-hydride diiron complex with a base-containing diphosphine ligand relevant to the [FeFe]-hydrogenase active site, Chem. Commun. 44 (2008) 5800–5802.
[35] S. Ezzaher, J.F. Capon, F. Gloaguen, F.Y. Petillon, P. Schollhammer, J. Talarmin, N. Kervarec, Influence of a pendant amine in the second coordination sphere on proton transfer at a dissymmetrically disubstituted diiron system related to the [2Fe](H) subsite of [FeFe]H(2)ase, Inorg. Chem. 48 (1) (2009) 2–4.

[36] F.F. Xu, C. Tard, X.F. Wang, S.K. Ibrahim, D.L. Hughes, W. Zhong, X.R. Zeng, Q.Y. Luo, X.M. Liu, C.J. Pickett, Controlling carbon monoxide binding at di-iron units related to the iron-only hydrogenase sub-site, Chem. Commun. 5 (2008) 606–608.
[37] M. Razavet, S.C. Davies, D.L. Hughes, C.J. Pickett, {2Fe3S} clusters related to the di-iron sub-site of the H-centre of all-iron hydrogenases, Chem. Commun. 9 (2001) 847–848.
[38] S. Friedrich, M. Schubart, L.H. Gade, I.J. Scowen, A.J. Edwards, M. McPartlin, Titanium and zirconium complexes containing a novel dianionic trifunctional amido ligand, Chem. Ber. 130 (12) (1997) 1751–1759.
[39] Y.W. Wang, Z.M. Li, X.H. Zeng, X.F. Wang, C.X. Zhan, Y.Q. Liu, X.R. Zeng, Q.Y. Luo, X.M. Liu, , Synthesis and characterisation of three diiron tetracarbonyl complexes related to the diiron centre of [FeFe]-hydrogenase and their protonating, electrochemical investigations, New J. Chem. 33 (8) (2009) 1780–1789.
[40] G.M. Sheldrick, SHELX-97-programs for crystal structure determination (SHELXS) and refinement (SHELXL), University of Göttingen, Germany, 1997.
[41] R. Ahlrichs, M. Bar, M. Haser, H. Horn, C. Kolmel, Electronic structure calculations on workstation computers: the program system turbomole, Chem. Phys. Lett. 162 (3) (1989) 165–169.
[42] A. Schafer, C. Huber, R. Ahlrichs, Fully optimized contracted Gaussian basis sets of triple zeta valence quality for atoms Li–Kr, J. Chem. Phys. 100 (8) (1994) 5829–5835.
[43] J.P. Perdew, Density-functional approximation for the correlation energy of the inhomogeneous electron gas, Phys. Rev. B 33 (12) (1986) 8822–8824.
[44] A.D. Becke, Density-functional exchange-energy approximation with correct asymptotic behavior, Phys. Rev. A 38 (6) (1988) 3098–3100.
[45] M. Bruschi, G. Zampella, P. Fantucci, L. De Gioia, DFT investigations of models related to the active site of [NiFe] and [Fe] hydrogenases, Coord. Chem. Rev. 249 (15–16) (2005) 1620–1640.
[46] L. Bertini, M. Bruschi, L. de Gioia, P. Fantucci, C. Greco, G. Zampella, Quantum chemical investigations of reaction paths of metalloenzymes and biomimetic models – the hydrogenase example, Atomistic Approaches Mod. Biol. (2007) 1–46.
[47] M. Bruschi, C. Greco, G. Zampella, U. Ryde, C.J. Pickett, L. De Gioia, A DFT investigation on structural and redox properties of a synthetic Fe_6S_6 assembly closely related to the [FeFe]-hydrogenases active site, C. R. Chim. 11 (8) (2008) 834–841.
[48] T. Helgaker, Transition-state optimizations by trust-region image minimization, Chem. Phys. Lett. 182 (5) (1991) 503–510.
[49] K. Eichkorn, F. Weigend, O. Treutler, R. Ahlrichs, Auxiliary basis sets for main row atoms and transition metals and their use to approximate Coulomb potentials, Theor. Chem. Acc. 97 (1) (1997) 119–124.
[50] A. Schafer, A. Klamt, D. Sattel, J.C.W. Lohrenz, F. Eckert, COSMO implementation in TURBOMOLE: extension of an efficient quantum chemical code towards liquid systems, Phys. Chem. Chem. Phys. 2 (10) (2000) 2187–2193.
[51] Z. Dang, Y. Yang, R. Ji, S. Zhang, Synthesis and antibacterial activity of novel fluoroquinolones containing substituted piperidines, Bioorg. Med. Chem. Lett. 17 (16) (2007) 4523–4526.
[52] Y.C. Sunil Kumar, M.P. Sadashiva, K.S. Rangappa, An efficient synthesis of 2-(1-methyl-1,2,5,6-tetrahydropyridin-3-yl)morpholine: a potent M1 selective muscarinic agonist, Tetrahedron Lett. 48 (26) (2007) 4565–4568.
[53] G. Zampella, M. Bruschi, P. Fantucci, M. Razavet, C.J. Pickett, L. De Gioia, Dissecting the intimate mechanism of cyanation of $\{2Fe_3S\}$ complexes related to the active site of all-iron hydrogenases by DFT analysis of energetics, transition states, intermediates and products in the carbonyl substitution pathway, Chem. Eur. J. 11 (2) (2005) 509–520.
[54] H.K. Hall, Correlation of the base strengths of amines1, J. Am. Chem. Soc. 79 (20) (1957) 5441–5444.
[55] H.K. Hall, Steric effects on the base strengths of cyclic amines1, J. Am. Chem. Soc. 79 (20) (1957) 5444–5447.
[56] E.A. Braude, F.C. Nachod, Determination of Organic Structures by Physical Methods, Academic Press, New York, 1962.
[57] L.G. Wade, Organic Chemistry, fifth ed., Prentice Hall, Upper Saddle River, NJ, 2003.
[58] P. Bonvicin, A. Levi, V. Lucchini, G. Scorrano, Acid-base behavior of sulfides, J. Chem. Soc., Perkin Trans. 2 15 (1972) 2267–2269.
[59] H. Sigel, V.M. Rheinberger, B.E. Fischer, Fischer, stability of metal ion/alkyl thioether complexes in solution. Ligating properties of "isolated" sulfur atoms, Inorg. Chem. 18 (12) (1979) 3334–3339.
[60] J. McMurry, Organic Chemistry, third ed., Brooks/Cole Pub., Pacific Grove, California, 1992.
[61] M. Bruschi, P. Fantucci, L. De Gioia, DFT investigation of structural, electronic, and catalytic properties of diiron complexes related to the [2Fe](H) subcluster of Fe-only hydrogenases, Inorg. Chem. 41 (6) (2002) 1421–1429.
[62] M. Bruschi, P. Fantucci, L. De Gioia, Density functional theory investigation of the active site of [Fe]-hydrogenases: effects of redox state and ligand characteristics on structural, electronic, and reactivity properties of complexes related to the [2Fe](H) subcluster, Inorg. Chem. 42 (15) (2003) 4773–4781.
[63] G. Zampella, C. Greco, P. Fantucci, L. De Gioia, Proton reduction and dihydrogen oxidation on models of the [2Fe](H) cluster of [Fe] hydrogenases. A density functional theory investigation, Inorg. Chem. 45 (10) (2006) 4109–4118.